*Int. J. Therm. Sci.* (2001) 40, 603–621

S1290-0729(01)01251-0/FLA

# Study of a macroscopic sliding contact thermal model from microscopic models

Patrice Chantrenne *, Martin Raynaud

*Centre de Thermique, ESA CNRS 5008, INSA de Lyon, Bât. 404, 20 Avenue Albert Einstein, 69621 Villeurbanne cedex, France*

(Received 13 January 2000, accepted 14 September 2000)

**Abstract** — The macroscopic sliding contact thermal model studied here involves two parameters: a sliding contact thermal resistance and a heat generation coefficient which can be determined from a microscopic model. For the two proposed microscopic models, the aim is to provide correlations which allow fast and easy determination of the two macroscopic parameters. The various definitions of the thermal resistance are also studied and our results are compared with other published work. The influence of the microscopic model on the macroscopic parameters is studied. It is shown that the heat generation coefficient depends on the location of the heat generated by friction. © 2001 Éditions scientifiques et médicales Elsevier SAS

**sliding contact / friction / thermal resistance / heat generation / macroscopic model / microscopic model**

**Résumé** — Cette étude concerne un modèle thermique macroscopique du contact glissant faisant intervenir deux paramètres : une résistance thermique de contact et un coefficient de génération de chaleur qui sont déterminés à partir de modèles microscopiques. L'objectif est d'obtenir des corrélations pour déterminer rapidement les deux paramètres. Deux modèles microscopiques sont proposés. Les différentes définitions de la résistance thermique sont discutées et nos résultats sont comparés avec la littérature. L'influence du modèle microscopique sur les paramètres macroscopiques est étudiée. Il est montré que le coefficient de génération de chaleur dépends de la répartition volumique de la chaleur générée par frottement. © 2001 Éditions scientifiques et médicales Elsevier SAS

**contact glissant / frottement / résistance thermique / génération de chaleur / modèle macroscopique / modèle microscopique**

## Nomenclature

| | | |
|---|---|---|
| $a$ | diffusivity | $m{\cdot}s^{-2}$ |
| $2B$ | periodicity of the defect | m |
| $2b$ | width of the defect | m |
| $cp$ | specific heat | $J{\cdot}kg^{-1}{\cdot}K^{-1}$ |
| $e$ | thickness | m |
| $H$ | height of the defect on the contacting surfaces | m |
| $h$ | height of the volume in which friction heat is generated | m |
| $h_{\text{infi}}$ | equivalent thermal conductance of the bulk solids ($i = 1, 2$) | $W{\cdot}K^{-1}{\cdot}m^{-2}$ |
| $g$ | fraction of the friction heat generated in the solid 1 | |
| $p$ | friction heat partition coefficient | |
| $R$ | thermal contact resistance | $m^2{\cdot}K{\cdot}W^{-1}$ |
| $T$ | temperature | °C |
| $\overline{T}$ | Time average temperature | °C |
| $T_{\text{infi}}$ | bulk temperature of solid $i$ ($i = 1, 2$) | °C |
| $w$ | width of the zone where friction heat occurs | m |

*Greek Symbols*

| | | |
|---|---|---|
| $\alpha$ | friction heat generation factor | |
| $\Delta t$ | time step | |
| $\Delta x$ | spatial step | |
| $\eta$ | fraction of thermal resistance | |
| $\bar{\eta}$ | space average fraction of thermal resistance | |
| $\varphi$ | heat flux | $W{\cdot}m^{-2}$ |
| $\bar{\varphi}$ | time average heat flux | $W{\cdot}m^{-2}$ |
| $\varphi_g$ | friction heat flux | $W{\cdot}m^{-2}$ |
| $\lambda$ | conductivity | $W{\cdot}m^{-1}{\cdot}K^{-1}$ |
| $\rho$ | density | $kg{\cdot}m^{-3}$ |

* Corresponding author.
*E-mail addresses:* patrice.chantrenne@cethil.insa-lyon.fr (P. Chantrenne), raynaud@cethil.insa-lyon.fr (M. Raynaud).

*subscripts*

| | |
|---|---|
| 1 | solid 1 |
| 2 | solid 2 |
| a | apparent (contact area) |
| c | contact |
| p | perfect contact |
| r | real (contact area) |
| sl | sliding contact |
| t | total |

*upperscript*

| | |
|---|---|
| a | asperity |
| b | bulk |
| L | Laraqi |

*dimensionless variable*

$V^* = \frac{V2B}{a}$

$H^* = \frac{H}{2B}$

$b^* = \frac{b}{B}$

$h^* = \frac{h}{2B}$

$R^* = \frac{R\lambda}{2B}$

## 1. INTRODUCTION

For engineering applications which involve sliding contact solids, it is important to know accurately the temperature of the contacting surfaces and the heat transfer rate between the contacting solids. This information is necessary to understand properly the mechanical and tribological behaviour of materials. To avoid many expensive and fastidious measurements, it is convenient to use a macroscopic sliding contact thermal model to predict the surface temperatures and heat fluxes values.

Two kinds of models were proposed in the literature. In the first one, it is assumed that the average temperatures of the contacting surfaces are equal. This model was first introduced around 1930 [1] and was then widely used [2–6]. It is then possible to calculate the temperature field in the contacting solids by using only one parameter, $p$, which is the friction heat partition coefficient (*figure 1*). $p$ is the fraction of the friction heat *which goes into* the solid 1. Actually, it has been shown that:

- $p$ depends on the contacting surface characteristics, on the macroscopic charasteristics and thermal boundary conditions of the contacting solids as well as the initial conditions [7].
- the two average temperatures of the contacting surfaces are not equal [8, 9]. This phenomenon has been studied first for static contact. To represent the temperature jump at the interface, a contact thermal resistance was introduced. This static contact resistance has been the subject of a large number of experimental and theoretical studies for steady and transient states [8, 10–14].

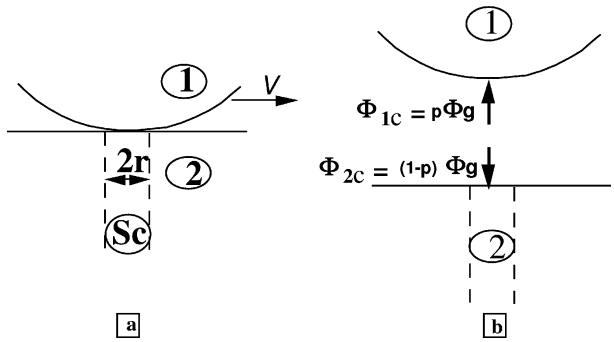


**Figure 1.** Macroscopic sliding contact thermal model involving the friction heat partition coefficient $p$; (a) reality, (b) model.

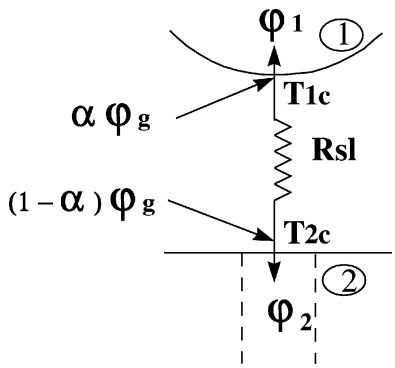


**Figure 2.** Macroscopic sliding contact thermal model involving a siding contact thermal resistance $R_{sl}$ and the friction heat generation coefficient $\alpha$.

Thus, by analogy with static contact, the second type of models assumes that there is a sliding contact thermal resistance, $R_{sl}$, between the two contacting surfaces. Sliding contact thermal resistance have been determined experimentally for journal bearing [15] and for forming [16–19]. The influence of the sliding velocity has been studied [20, 21].

But when friction heat is large, it is necessary to use another thermal model. It involves the sliding contact thermal resistance and another parameter for the friction heat. For this second parameter, Bardon [8] introduced the friction heat generation factor, $\alpha$, which is usually interpreted as the fraction of the friction heat *generated at the surface* of the solid 1. The complementary part is generated at the surface of the solid 2 (*figure 2*). A global energy balance and an energy balance at the surface of

the solid 1 allow to obtain the two equations which are needed to describe the boundary condition of the two contacting solids:

$$\varphi_g = \varphi_1 + \varphi_2, \quad (1)$$

$$\varphi_1 = \alpha\varphi_g + \frac{(T_{c2} - T_{c1})}{R_{sl}} \quad (2)$$

It must be noted that there is no need to consider the friction heat generation factor to couple the two contacting solids *when the heat transfer from one solid to the other one is much greater than the friction heat*. It happens for example for stamping or forging operations when the difference between the bulk temperature of the two contacting solids is high; even if heat is generated by friction and plastic deformation, it is much smaller than the heat transferred between the two solids. It means that $\varphi_g$ is negligible compared to $|\varphi_1|$ and $|\varphi_2|$. Then equation (1) becomes:

$$\varphi_1 = -\varphi_2$$

Similarly, in equation (2), $\alpha\varphi_g$ can also be neglected compared to the flux that crosses the interface. Then the temperature jump between the two contacting surfaces do not depend on $\alpha$ but *still depends on the sliding contact thermal resistance* $R_{sl}$:

$$(T_{2c} - T_{1c}) = \varphi_1 R_{sl}$$

The friction heat generation factor must be taken into account only when the friction heat has a great influence on the contact temperatures. This occurs when the initial bulk temperatures of the contacting solids are similar like in ball bearings, brakes, gears, during metal cutting, etc.

Instead of $R_{sl}$ and $\alpha$, Laraqi [22] proposed two other parameters to describe the friction heat generation. He assumes that the contact interface profile varies with a gaussian distribution and that the friction heat is generated at the contact interface. So the friction heat follows the same gaussian distribution than the contact interface location. His model is also based on two parameters which depend only on the contacting surface characteristics and not on the macroscopic geometry of the solids or boundary conditions.

Our study is focused on the thermal model proposed by Bardon [8] involving the two parameters $R_{sl}$ and $\alpha$. The aim is to give correlations to calculate $R_{sl}$ and $\alpha$ and to study the influence of the microscopic parameters (the surface roughness, the thermal properties, the sliding velocity and heat generation parameters). Such correlations are useful for a quick and easy evaluation of the thermal resistance and the friction heat generation factor that are needed for the macroscopic modelling of systems which have solids in contact.

As the two macroscopic parameters $R_{sl}$ and $\alpha$ depend on the microscopic geometry of the contacting surfaces, the correlations which are obtained depend on the microscopic model of the contacting surfaces. In the first part, two microscopic models of the contacting interface are proposed. These two models are different. The first one considers a rough surface sliding on a perfectly smooth surface. For the other, the two sliding surfaces are rough. The numerical methodology to determine parameters $R_{sl}$ and $\alpha$ is recalled. In the second part, $R_{sl}$ is determined as a function of the microscopic parameters for the two models which are compared. The last part concerns the determination of $\alpha$ as a function of the microscopic parameters. Assuming that the friction heat is generated in a volume instead of being localised at the contact interface, it is shown that the microscopic parameters that describe the heat generation has a non negligible influence on $\alpha$.

## 2. MICROSCOPIC ANALYSIS

Two microscopic models are considered here:

- one named S/R model: a smooth surface is sliding on a rough 2D surface so the contact between the two solids is continuous.
- the other, named R/R model: a rough 2D surface is sliding on a rough 2D surface. The contact between the two surfaces can be discontinuous which is the most interesting difference with the S/R model.

It is not an easy task to model surface geometry and it has been tackled a long time ago for thermal and mechanical applications. The main interest for thermal application is the determination of the real contact area to predict the static thermal contact resistances. The geometry of the contacting surfaces is usually 3D and the shape of the asperity cannot be easily described with simple functions so most of the time statistical considerations are used to define characteristic lengths or parameters [23–25]. In this study, to avoid complexity and to allow the implementation of simple numerical solutions (for the thermal field calculations), it is assumed that the surface defects have square periodic shapes. It is not intended to accurately represent real contacting surfaces because the aim is to illustrate the determination methodology of $R_{sl}$ and $\alpha$ and to point out the influence of the various parameters (surface roughness, sliding velocity, etc.).

Still, this approximation is valid when the surfaces are turned so that the defects can be considered periodic and

infinite in one direction. Such a surface has been scanned and its profile has been plotted on *figure 3(a)*. As usual, the scale in the $x$ direction allows to represent a much greater length than in the $y$ direction. In these conditions, it is not obvious to determine the shape's defect. The profile is plotted on *figure 3(b)* with a different scale in the $x$ direction to point out the real shape of the defects. It appears that the real profile can easily be fitted with a square periodic profile, which, in this case, is a good approximation. This model does not represent the smaller defects but it is not necessary because the typical length of these smaller defects (10 µm) is one order of magnitude less than the typical length of the square periodic profile (150 µm). So, the contribution to the total constriction resistance due to the smaller defects is negligible toward the constriction resistance due to the main defect [8].

## 2.1. Smooth to Rough (S/R) microscopic model

Let consider a solid 1 sliding on a solid 2 with the velocity $V$. The contact at the macroscopic scale is shown on *figure 4(a)*. At this scale, heat transfer are described by the macroscopic model which involve the two parameters: $R_{\mathrm{sl}}$ and $\alpha$ (*figure 2*). At the microscopic scale it can be modelled by a geometry such as the one of *figure 4(b)*. The two solids are supposed to be infinite in the $x$ and $z$ directions. Note that, similarly to *figure 3(b)*, *figure 4* is not to scale. Typically, $b^* = \frac{b}{B} < 0.1$ and the order of magnitude of $H$ is the µm. The surface of solid 1 is perfectly smooth. The contacting surface of the solid 2 is modelled with periodic defect. So the study can be limited to one elementary cell as shown by *figure 4(c)*. The spatial periodicity is $2B$, the height and the width of the defect are equal to $H_2$ and $2b_2$, respectively. The thickness of the elementary cell, defined by $e_1 + e_2$, is chosen so that the thermal constriction in the solids (due to the surface defect) is fully developed. This condition is satisfied when the distance between the defect and the cell boundary is at least greater than the periodicity of the defect. This model and the numerical solution to calculate the temperature field were already presented in [28].

## 2.2. Rough to Rough (R/R) microscopic model

The principle of the model is shown by *figures 5(a)–(c)*. It is similar than for the S/R model except that for this model, the two contacting surfaces are made of periodic defects. The spatial periodicity is $2B$ for the two solids. For the solid $i$ $(i = 1, 2)$ the height and the width of the defects are equal to $H_i$ and $2b_i$ respectively and the two solids are still supposed to be infinite in the $x$ and $z$ directions. Once again, this figure is not to scale. The relative sliding velocity is equal to $V$. A numerical solution, using finite difference method, has been implemented to calculate the temperature field in the solids. It is not presented here but it uses the same kind of governing equation than for the S/R model. There is one more difficulty for the numerical solution because the geometry of the contacting interface changes with time. The mesh is presented on *figure 5(d)*. The spatial step in the $x$ direction and the time step is chosen so that $\Delta x = V \Delta t$.

As for the R/R model, the thicknesses $e_1$ and $e_2$ are chosen large enough so that the temperature field is 1-D near the upper and lower boundaries of the elementary cells. However, these temperatures at the boundary vary with time depending on the frequency of the thermal perturbation due to the contacting solids. The pulsation, $\omega$, is:

$$\omega = \frac{2\pi V}{2B} \tag{3}$$

For high thermal diffusivity and low pulsation, the periodic perturbation may not be completely damped at the cell boundaries. As the instantaneous values of the temperature and heat flux periodically vary with time, only their average over a time period ($\overline{T}_1$ and $\overline{T}_2$ for the temperature and $\bar{\varphi}$ for the heat flux) are used. This is valid since our objective is to find parameters of macroscopic model. Thus instantaneous values which are related to the macroscopic model are not of interest for the present study.

## 2.3. General considerations

The case of dry sliding contact is considered, i.e., there is no lubricant and the two solids are in direct contact. In the present study, the convective and conductive heat transfer of the gas captured between the defects are not taken into account. Moreover, for most practical cases, the radiative heat transfer between the cavities surfaces can be neglected [26].

The density $\rho_i$, the specific heat $cp_i$ and the thermal conductivity $k_i$ of the two solids are known. They do not vary with temperature. The elementary cell of thickness $e_1 + e_2$ exchanges heat with the bulk of the solids. The heat thermal conductance and bulk temperatures are $h_{\mathrm{inf}1}$, $T_{\mathrm{inf}1}$ and $h_{\mathrm{inf}2}$, $T_{\mathrm{inf}2}$.

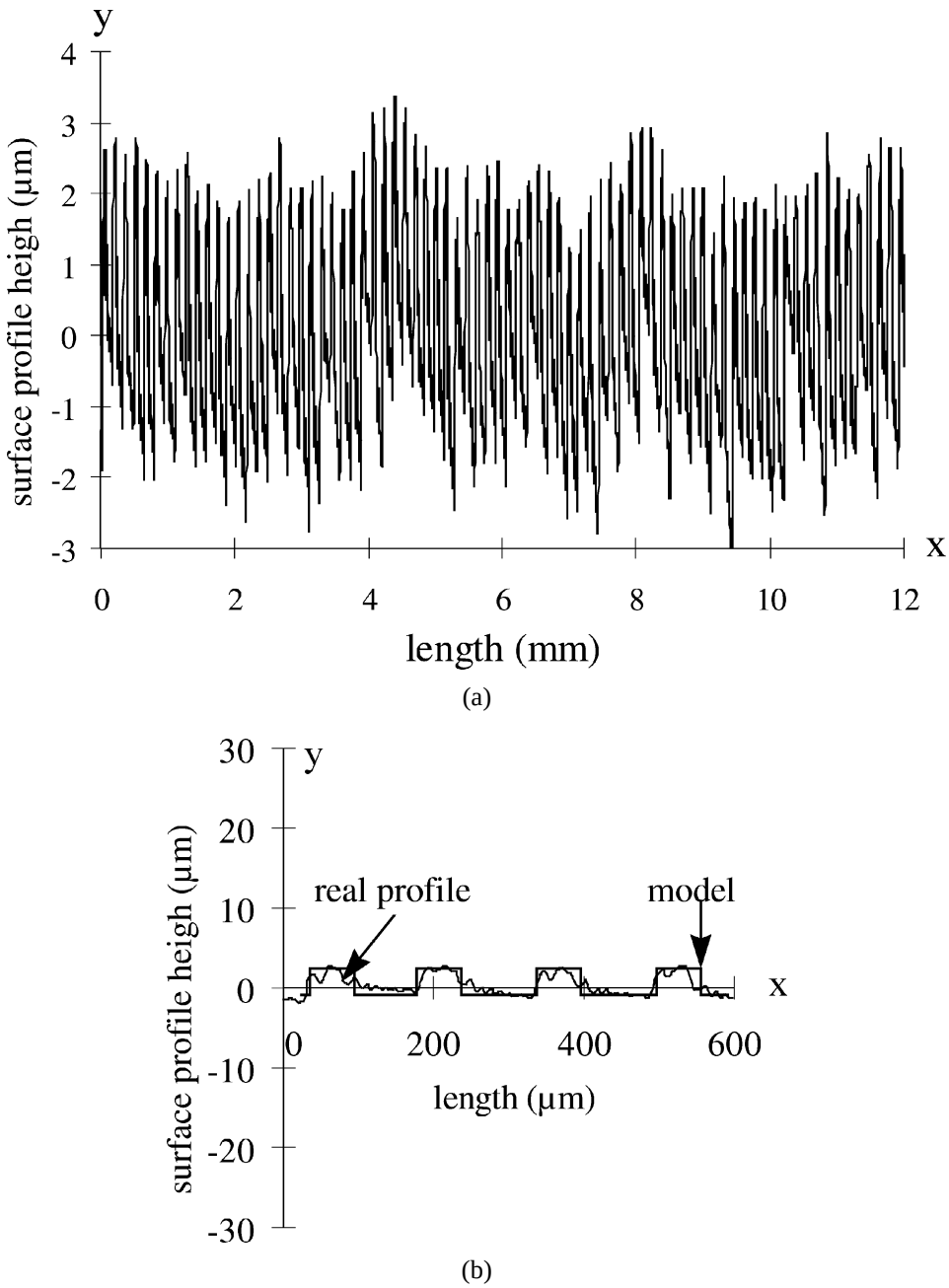


**Figure 3.** Profile of a turned surface plotted using the usual scale ratio between the $x$ and $y$ direction (a) and then a smaller scale ratio (b) to point out the defects shape.

The friction heat is due to several physical phenomena [27] and it is always generated in a volume even if this volume is very small (some atomic layers). Herein, a volumic friction heat is considered (*figures 4* and *5*). To simplify the numerical model a simple geometry of the volume in which friction heat is generated has been chosen. The aim is to show that it is important to take into account a volumic friction heat generation. The functions $g_1$ and $g_2$ are used to characterise the variation of the spatial friction heat. When physical phenomena are known

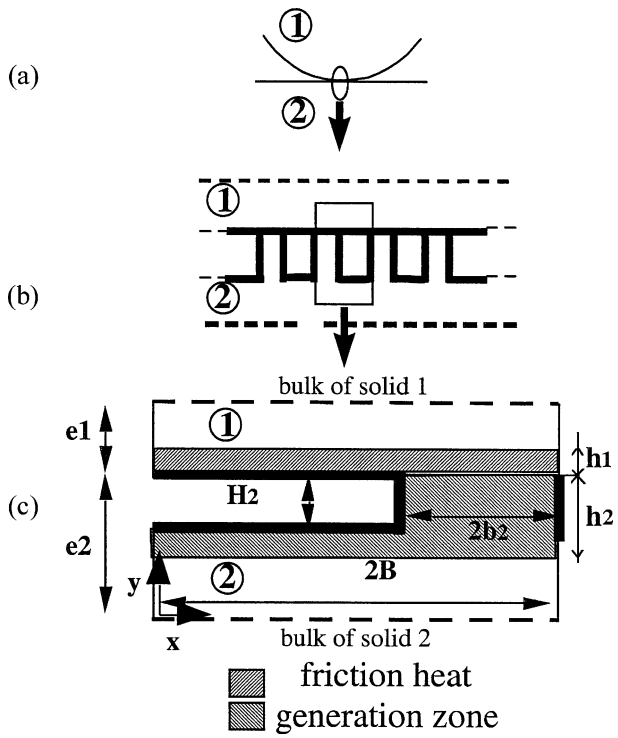


**Figure 4.** Smooth to Rough microscopic contact thermal model: (a) Macroscopic scale; (b) Microscopic scale; (c) Elementary cell.

functions $g_1$ and $g_2$ could be realistic and complicated. Actually, it is very hard to find models describing friction heat generation in solids except for metal forging and stamping [29]. As they are usually not known, $g_1$ and $g_2$ will later be considered as constants: $g$ and $(1-g)$. The parameter $g$ is then the fraction of the friction heat *generated within the solid* 1, while the complementary part $(1-g)$ of the friction heat is generated within the solid 2. As explained in [28], $g$ must not be mistaken for $p$.

As shown on *figures 4* and *5*, it is supposed that the friction heat localisation is different for the R/R and S/R models. It is done on purpose to show that the methodology does not depend on the way the friction heat is generated. For the R/R model, it is assumed that the friction heat is generated in a volume *just under the real contact area*. This volume is defined by the two height $h_i$ and the two width $w_i$ ($i = 1, 2$ for solid 1 and 2). One define $h$ as the distance (in the $y$ direction) between the theoretical interface and a point in the solid 1 or 2. For $h \leq h_i$ $w_i$ is constant, but it depends on time because the width of the real contact depends on the relative position of the defect. For $h > h_i$, $w_i$ is equal to zero. Thus the

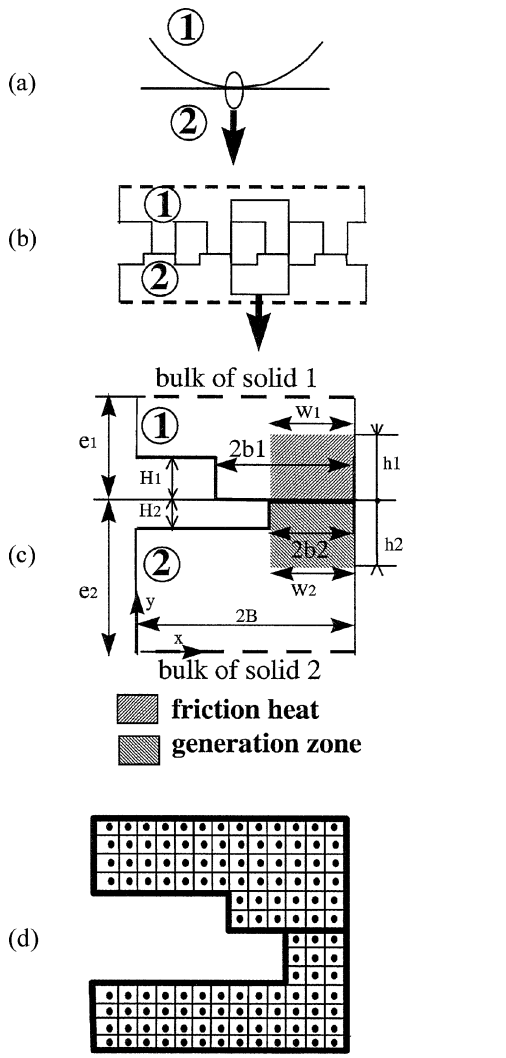


**Figure 5.** Rough to Rough microscopic contact thermal model: (a) Macroscopic scale; (b) Microscopic scale; (c) Elementary cell; (d) Mesh used for the numerical solution.

frictional heat is also time dependent:

$$\varphi_g(t) = \frac{1}{2B}\left[w_1(t)\int_0^{h_1} g_1(h)\,\mathrm{d}h + w_2(t)\int_0^{h_2} g_2(h)\,\mathrm{d}h\right] \quad (4)$$

but the mean value of $\varphi_g(t)$, $\varphi_g$ is equal to:

$$\varphi_g = \frac{1}{2B}\left[\bar{w}_1\int_0^{h_1} g_1(h)\,\mathrm{d}h + \bar{w}_2\int_0^{h_2} g_2(h)\,\mathrm{d}h\right] \quad (5)$$

where $\bar{w}_1$ and $\bar{w}_2$ are the mean value of $w_1(t)$ and $w_2(t)$ over a period of time.

For the S/R model, *heat is generated under the whole apparent contact area*. The width $w_i$ does not depend on

time but depends on the value of $h$: $w_1 = 2b_1$ if $h \leq H_1$, $w_1 = 2B$ if $h > H_1$ and $w_2 = 2B$. Thus the frictional heat is:

$$\varphi_g = \frac{1}{2B}\left[\int_0^{h_1} g_1(h)w_1(h)\,\mathrm{d}h + \int_0^{h_2} g_2(h)w_2(h)\,\mathrm{d}h\right] \tag{6}$$

The conservation of energy implies that the heat flux at the two surfaces $x = 0$ and $x = 2B$ must be equal to satisfy the spatial periodicity. Using the numerical solutions, the temperature field can be calculated at steady state for the S/R model and during the periodic state for the R/R model. The finite difference mesh was refined until the solution becomes independent of the mesh.

## 2.4. Numerical methodology for the determination of $R_{sl}$ and $\alpha$

### 2.4.1. Determination of the contact thermal resistance

This methodology has already been given in [28] but it is briefly recalled here to show how it is applied to the R/R model.

To determine $R_{sl}$, the temperature field of the microscopic model is calculated for the specific case of no friction heat. The contact thermal resistance is independent of the friction heat since the thermophysical properties are constant. Thus the special case of zero friction heat can be used to determine $R_{sl}$ from equation (2) by setting $\varphi_g = 0$.

The two macroscopic contact temperatures $T_{1c}$ and $T_{2c}$ can be obtained by extrapolating the far field temperature (which is 1-D if the thicknesses are big enough as explained in Section 2.1) toward the interface of contact. This is done using the Fourier's Law and upper and lower cell boundaries temperatures $T_i$:

$$T_{ic} = T_i + \varphi_i \frac{e_i}{\lambda_i}, \quad i = 1, 2 \tag{7}$$

For the S/R model, the *steady state temperatures* of the cell boundaries, $T_1$ and $T_2$, and the conductive flux, $\varphi$ (calculated from the numerical solution by using the boundary condition on the cell boundary either for solid 1 or solid 2), are used to calculate $R_{sl}$. For the R/R model, it is the time average of the temperatures and heat flux over a time period ($\overline{T}_1$, $\overline{T}_2$ and $\overline{\varphi}$) which are considered.

### 2.4.2. Determination of the friction heat generation factor

Once the thermal contact resistance is determined, the friction heat factor can be determined from equation (2). It is only required to calculate the temperature distribution of the two contacting solids with a non zero friction heat. $\varphi_1$ is calculated from the temperature field in the solid 1 and the two contact temperatures $T_{1c}$ and $T_{2c}$ are obtained from equation (7).

For the S/R model, $T_{1c}$, $T_{2c}$ and $\varphi_1$ are the steady state values while for the R/R model, they must be the mean values calculated over a time period.

## 3. STUDY OF THE SLIDING CONTACT THERMAL RESISTANCE

### 3.1. Correlation

The aim is to develop a simple correlation for $R_{sl}$. It will allow to determine quickly $R_{sl}$ and study the influence of the various microscopic parameters of the model. A dimensional analysis was carried out to find which dimensionless parameters influence the sliding contact resistance. $R_{sl}$ depends on the following microscopic parameters:

- $2B$, the spatial periodicity,
- $H_i$ and $2b_i$, the heigh and the width of the defects,
- $\lambda_i$, $\rho_i$, $cp_i$ the thermophysical properties of the solids,
- $V$ the relative sliding velocity.

So three independent parameters appeared:

- $V_i^* = \frac{V 2B\rho_i cp_i}{\lambda_i}$ the dimensionless sliding velocity,
- $H_i^* = \frac{H_i}{2B}$ the dimensionless height,
- $b_i^* = \frac{b_i}{B_i}$ the dimensionless width.

The sliding contact thermal resistance is the sum of the sliding contact thermal resistance due to solid 1 and solid 2:

$$R_{sl} = R_{sl1} + R_{sl2} \tag{8}$$

Each thermal resistance is equal to a characteristic dimension of the system multiplied by a dimensionless thermal resistance divided by the conductivity of the solid [30]:

$$R_{sli} = \frac{\delta R_{sli}^*}{\lambda_i} \tag{9}$$

The characteristic dimension of the system is chosen as the spatial periodicity of the geometry, $\delta = 2B$. In the

next section correlations are given for the dimensionless thermal resistances.

### 3.1.1. Correlations for the S/R model

In solid 2, the constriction from the external surface toward the defects is not influenced by the velocity of solid 1. The velocity affects the temperature gradient within the defect but its influence is limited to the real contact area. This later phenomenon has a very small effect on the thermal contact resistance compared to the constriction toward the defects. Consequently, the thermal resistance of solid 2 can be considered independent of the sliding velocity (it was verified by the calculations):

$$R^*_{\mathrm{sl2}} = R^*_{\mathrm{sl2}}\left(H^*_2, b^*_2\right) \tag{10}$$

Since solid 2 is smooth, its resistance is equal to a static constriction resistance, which depends on the dimensionless width $b^*$, multiplied by a function of the sliding velocity [20]:

$$R^*_{\mathrm{sl1}} = R^*_{\mathrm{st1}}\left(b^*_2\right) F\left(V^*_1\right) \tag{11}$$

Values of $R_{\mathrm{sl}}$ were calculated with the numerical solution of the microscopic model for several sets of values for the three microscopic dimensionless parameters:

– $H^*_2, b^*_2$ in the range $[0.05, 0.9]$ and

– $V^*_1$ in the range $[0, 200]$.

It was then possible to identify the three correlations $R^*_{\mathrm{sl2}}(H^*_2, b^*_2)$, $R^*_{\mathrm{st1}}(b^*_2)$ and $F(V^*_1)$:

$$R^*_{\mathrm{sl2}} = \left(\frac{1}{b^*_2} - 1\right) H^*_2 + \left(a_1 b^*_2 + a_2\right) \ln\left(\frac{1}{b^*_2}\right), \tag{12}$$

$$R^*_{\mathrm{sl1}} = \left(a_1 b^*_2 + a_2\right) \ln\left(\frac{1}{b^*_2}\right) \times \left(\frac{1 - \exp(-(a_3 V^*_1)^{a_4})}{(a_3 V^*_1)^{a_4}}\right) \tag{13}$$

with: $a_1 = -0.234$, $a_2 = 0.2847$, $a_3 = 0.07$, $a_4 = 0.7$.

Where $a_1$ to $a_4$ are calculated to fit the numerical results. The sliding contact thermal resistance is then calculated from equations (8), (9), (12) and (13). The difference between the values calculated with the numerical solution and with the correlation is less than 20%.

### 3.1.2. Correlation for the R/R model

To calculate $R_{\mathrm{sl1}}$ and $R_{\mathrm{sl2}}$, $R_{\mathrm{sl}}$ was first determined by using the same geometry and thermophysical properties for the two solids. In this case the microscopic dimensionless parameters, thus the thermal sliding resistances due to the two solids are equal:

$$R_{\mathrm{sl1}} = R_{\mathrm{sl2}} = \frac{R_{\mathrm{sl}}}{2} \tag{14}$$

Values of $R_{\mathrm{sl}}$ were calculated with the numerical solution of the microscopic model for several sets of values for the microscopic dimensionless parameters:

– $H^*_2, b^*_2, H^*_1, b^*_1$ in the range $[0.05, 0.9]$ and

– $V^*$ in the range $[0, 100]$. For computational time reasons, larger values of $V^*$ were not studied.

The proposed correlation for the dimensionless sliding contact thermal resistance is:

$$R^*_{\mathrm{sli}} = c_1\left(\frac{1}{b^*_i} - 1\right) H^*_i + c_2\left(\frac{1}{b^*_i} - 1\right)^{c_3} \left(V^*\right)^{c_4} \tag{15}$$

with: $c_1 = 0.93$, $c_2 = 0.4$, $c_3 = 1.45$, $c_4 = -0.24$.

Value of $c_1$ to $c_4$ are determined by fitting the numerical results. Numerical results showed that when the geometry and thermophysical properties are different for the two solids the above correlation is still correct. This can be explained by the fact that the constriction from the external surface toward the defects of one solid are weakly influenced either by the shape of the defects or by the thermophysical properties of the other solid.

The sliding contact thermal resistance is calculated from equations (8), (9) and (15). The difference between results from numerical solution and from the correlation is less than 20%.

## 3.2. Comparison of the two microscopic models

The sliding contact thermal resistance given by the two microscopic models are now compared to study the influence of the surface roughness.

For the S/R and R/R models, the solids are considered to be made of steel (one of the widely used material for gear and bearings) which thermophysical properties are:

$$\lambda_1 = \lambda_2 = 15\,\mathrm{W{\cdot}m^{-1}{\cdot}K^{-1}},$$
$$\rho_1 = \rho_2 = 7700\,\mathrm{kg{\cdot}m^{-3}},$$
$$cp_1 = cp_2 = 150\,\mathrm{J{\cdot}kg^{-1}{\cdot}K^{-1}}$$

The period of the defect is $2B = 10\ \mu\mathrm{m}$.

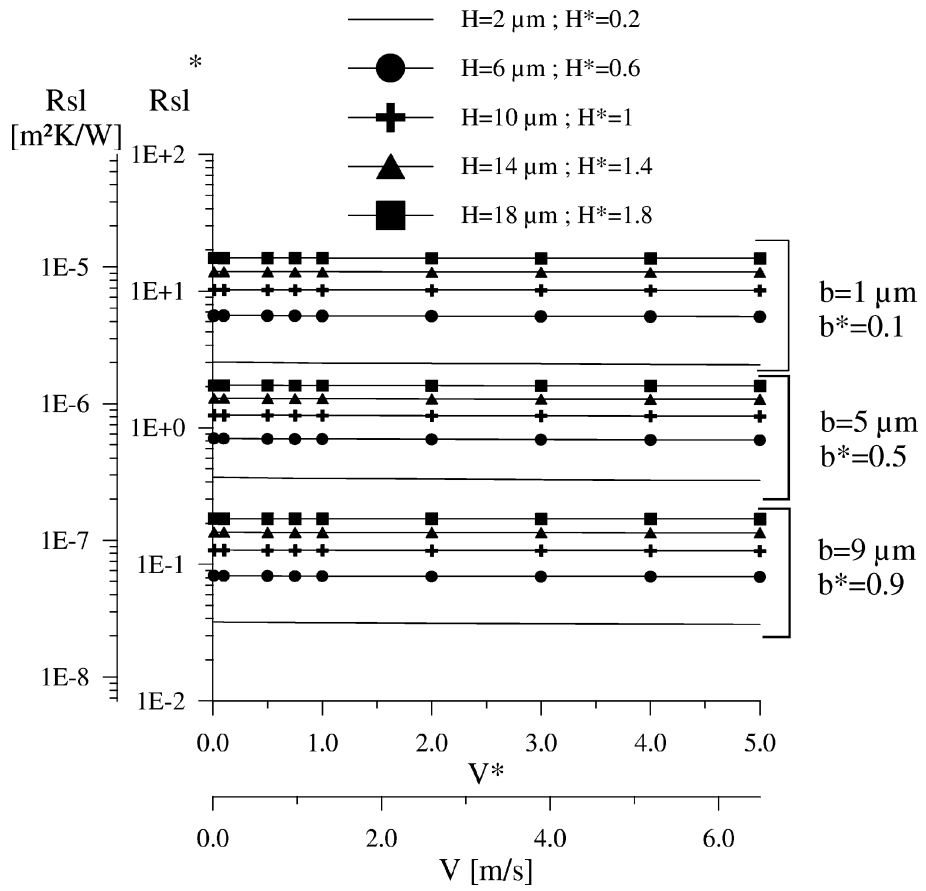


**Figure 6.** Variation of the sliding contact thermal resistance with the sliding velocity for different values of the width an height of asperities for the S/R model.

For the R/R model the defects of the two solids have the same width and height:

$$b_1 = b_2 = b; \qquad H_1 = H_2 = H$$

In order to compare the results of the two models, the width of the defect is the same for the S/R and the R/R models and the height of the defect of the S/R model is equal to the total height of the defects of the R/R model:

$$b_{S/R} = b_{R/R} \quad \text{and} \quad H_{S/R} = 2H_{R/R}$$

Results are plotted on *figures 6* and *7* for the S/R and R/R models, respectively. The sliding contact thermal resistance, $R_{sl}$, is shown versus the sliding velocity for different values of the width and height of the defects. The dimensionless values of the parameters are also given so that the results can be used for different values of the periodicity and thermal properties. Logically, the resistance decreases when the contact width increases and when the defects height decreases. Results are plotted for $b^* = 0.1$, 0.5 and 0.9. Practically surfaces with $b^* > 0.1$ are seldom encountered. Larger values were studied on purpose to better understand the phenomenon.

$R_{sl}$ ranges between $2{\cdot}10^{-8}$ $m^2{\cdot}K{\cdot}W^{-1}$ and $10^{-5}$ $m^2{\cdot}K{\cdot}W^{-1}$ for the S/R model and between $2{\cdot}10^{-8}$ $m^2{\cdot}K{\cdot}W^{-1}$ and $5{\cdot}10^{-5}$ $m^2{\cdot}K{\cdot}W^{-1}$ for the R/R model. With the R/R model, the real contact area is always smaller than the area of the defects, and, depending on the value of $b_i^*$, the contact can even be intermittent (for example when $b_i^* < 0.5$). This is why the thermal contact resistance obtained with the R/R model is always larger than the one obtained with the S/R model. The bigger the width of the defect, the smaller the difference between the two models. This is logical since the two resistances should be equal when $b^* = 1$. The variations of $R_{sl}$ with the sliding velocity are much more important for the R/R model ($R_{sl}$ can decreases by more than 600% when the sliding velocity increases) than for the S/R model (for the

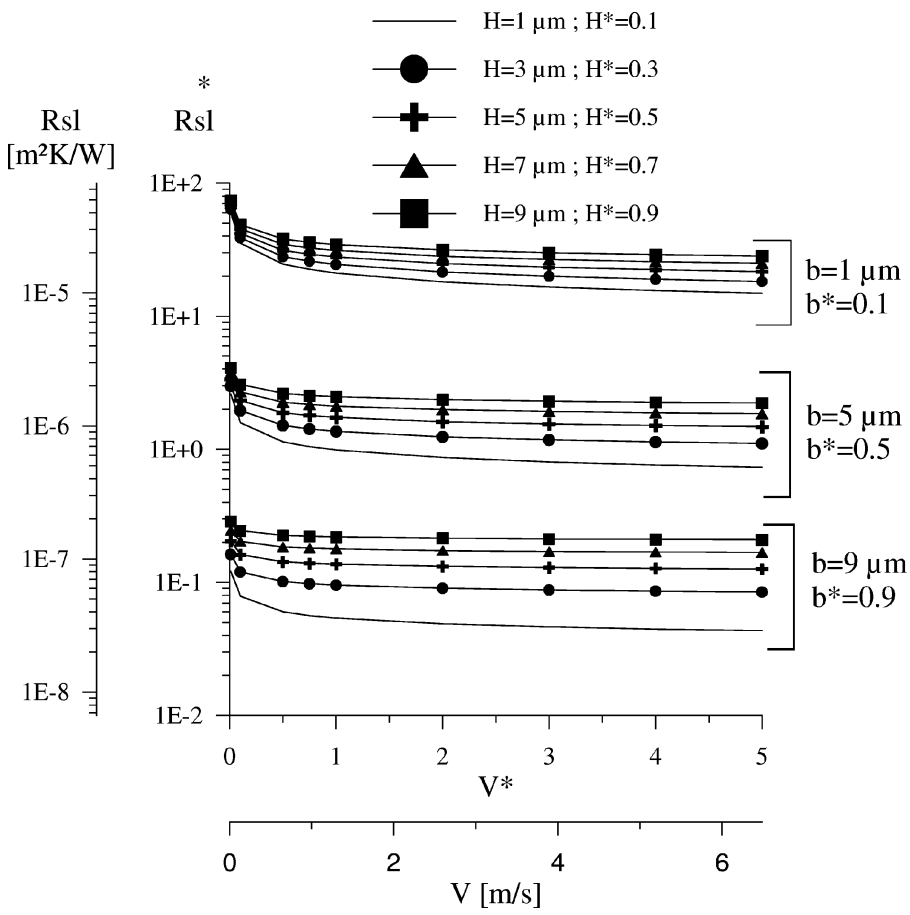


**Figure 7.** Variation of the sliding contact thermal resistance with the sliding velocity for different values of the width an height of asperities for the R/R model.

case studied, the sliding velocity has almost no influence on $R_{sl}$). It can be explained since the thermal contact resistance of the S/R model is mainly due to the presence of the defect in the solid 1 which is fixed and thus not influenced by the velocity.

## 3.3. Comparison with literature results

The aim of this section is to validate the determination of $R_{sl}$ obtained from the numerical solutions of the microscopic models. The proposed methodology allows to determine the sliding contact thermal resistance between two contacting solids but such data are seldom reported in the literature, except from experimental studies. Moreover the comparison with experimental results is difficult because the surface geometry or thermal properties of material are not well known and most of the works were done to determine the resistance for *static* contact instead of *sliding* contacts [15, 20].

### 3.3.1. Comparison with Laraqi [21]

Laraqi [21] studied the influence of the sliding velocity on the constriction resistance in a solid submitted to moving heat source bands (*figure 8*). He used the definition of the constriction resistance which states that, for semi-infinite solids submitted to surface heat sources, the constriction resistance is equal to:

$$R_{cs} = \frac{\overline{T}_r - \overline{T}_a}{\varphi} \tag{16}$$

Which is true only if the surfaces which are not submitted to the heat source are adiabatic. $\overline{T}_r$ is the mean temperature of the real contact area (under the surface sources), $\overline{T}_a$ is the mean temperature of the apparent contact area

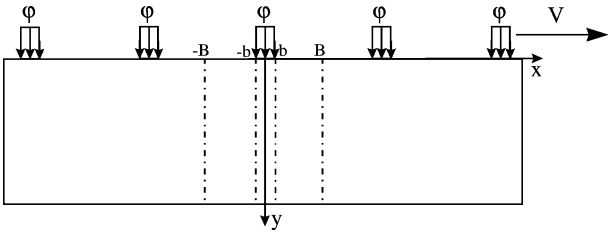


**Figure 8.** Solid submitted to periodic moving heat sources. Model studied by Laraqi to determine the constriction resistance as a function of the sliding velocity.

(total area) and $\varphi$ is the heat flux entering into the solid. He developed an analytical relation for the constriction resistance:

$$R_{cs}^{L} = \frac{2B\sqrt{2}}{2\lambda\pi^3 b^{*2}} \sum_{p=1}^{\infty} \frac{\sin^2(p\pi b^*)}{p^3} \times \sqrt{\frac{1}{\sqrt{1+(V^*/(2p\pi))^2}} + \frac{1}{1+(V^*/(2p\pi))^2}} \tag{17}$$

The non dimensional constriction resistance is then equal to:

$$R_{cs}^{L^*} = R_{cs}^{L} \frac{\lambda}{2B} \tag{18}$$

It can be compared to the thermal contact resistance due to the solid 2 of the S/R microscopic model. Comparison is done for the following geometry and thermophysical properties:

$2B = 0.003$ m; $2b = 0.0006$ m;

$H = 0.0006$ m; $V = 0.013$ m·s;

$\lambda_1 = \lambda_2 = 15$ W·m$^{-1}$·K$^{-1}$;

$\rho_1 = \rho_2 = 7700$ kg·m$^{-3}$;

$cp_1 = cp_2 = 150$ J·kg$^{-1}$·K$^{-1}$.

*Table I* gives the value of $R_{sl2}$ calculated using:

– the correlation obtained in the previous section, equations (13) and (9),

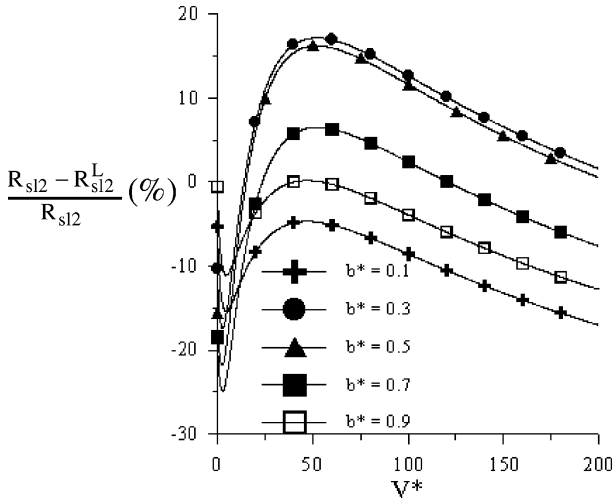


**Figure 9.** Difference in % between the constriction resistance in solid 2 for the S/R model and the values calculated with an analytical relation proposed by Laraqi [20] for the same geometry.

– the analytical solution proposed by Laraqi, equation (17),

– the microscopic S/R model and the definition of the thermal contact resistance used by Laraqi, equation (16). This is possible since the numerical solution of the thermal model allows to calculate the temperatures $\overline{T}_r$ and $\overline{T}_a$ of the solid 2 surface and the heat flux $\varphi$ that crosses the contact interface.

For this particular case, the differences between the values do not exceed 15%.

On *figure 9*, the relative difference between the results given by the correlation and those obtained with the analytical solution of Laraqi is shown as a function of the non dimensional sliding velocity for different values of $b^*$. It does not exceed 25%. Four main reasons allow to explain the differences:

– the two thermal models are not identical. As a matter of fact, the distribution of the heat flux on the real area of contact are not the same. In Laraqi's model, the heat flux is imposed and homogeneous: the flux is normal to the surface. In the present study this flux is not imposed,

TABLE I
Value of the thermal contact resistance due to solid 2 for the S/R microscopic model, calculated by three different means.

| Microscopic model value from the correlation | Microscopic model definition used by Laraqi | Analytical solution |
|---|---|---|
| $R_{sl2} = 6.51{\cdot}10^{-5}$ m$^2$·K·W$^{-1}$ | $R_{sl2} = 7.18{\cdot}10^{-5}$ m$^2$·K·W$^{-1}$ | $R_{sl2} = 7.71{\cdot}10^{-5}$ m$^2$·K·W$^{-1}$ |

i.e., the heat flux is not homogeneous and the flux lines are not necessarily normal to the surface of contact.

– the definitions used to calculate the thermal constriction resistances are not identical. This should not have a strong influence since $e_1$ and $e_2$ are large enough but it is difficult to quantify.

– our numerical correlation is not perfect since it comes from a fit of data points.

– numerical errors (round off and truncation) affecting the temperature field calculated with the numerical solution of the microscopic S/R model influence the value of the thermal contact resistance obtained from the temperature field.

### 3.3.2. Comparison with Vullierme et al. [20]

Experimental measurements of the constriction resistance as a function of the sliding velocity were carried out by Vullierme et al. [20] with a geometry very similar to the S/R microscopic model. Measurements were done for $2B = 0.00458$ m and $2b = 0.00092$ m. As the conductivity of the material (steel) was not given in the reference, it has been determined so that the thermal resistance obtained from the correlation (equations (13) and (9)) for the static contact (sliding velocity equal to 0) is equal to the static thermal resistance measured by Vullierme. A conductivity $\lambda = 36$ W·m$^{-1}$·K$^{-1}$ was found, which is in the range of the conductivity for steel. For the other sliding velocity ($V^* = 10$, 20, 40 and 80) the agreement between the experimental results and the value of $R_{sl2}$ obtained from the correlation (equations (13) and (9)) is very good (*figure 10*).

## 3.4. Conclusion

The sliding contact thermal resistance of the two models, for the same total height and width of defect, are really different especially for small sliding velocity and small ratio of real to apparent contact area (small $b^*$). A physical analysis of heat transfer through the two solids leads to correlations that can be used to predict thermal contact resistances. It was also possible to identify the part of the sliding contact resistance due to each solid. For the S/R model, the thermal resistance due to the smooth solid was compared to value given in the literature using a different definition of the thermal resistance (definition available for a semi infinite solid submitted to moving uniform heat source). There is no significant differences.

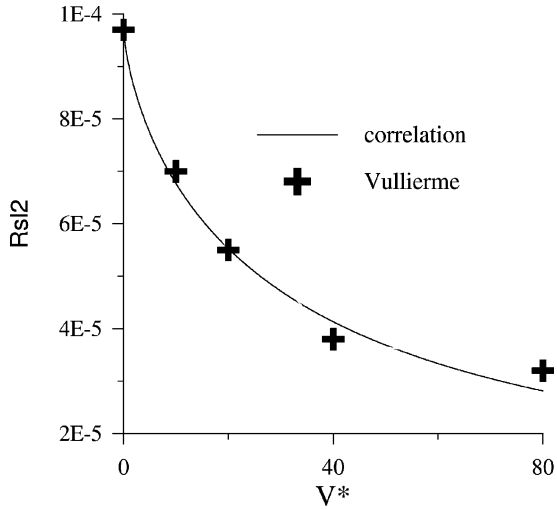


**Figure 10.** Influence of the sliding velocity on the constriction resistance in solid 2 of the S/R model. Comparison between experimental results (Vullierme et al. [24]) and the correlation (equations (16) and (12)).

## 4. STUDY OF THE FRICTION HEAT GENERATION COEFFICIENT

The other thermal contact parameter, the heat generation coefficient $\alpha$, is now studied.

For the first analytical analysis, Bardon [8] assumed that the friction heat is generated at the contact interface, *figure 11(a)*. The equivalent thermal resistance network is shown *figure 11(b)*. An analytical expression for the heat generation coefficient $\alpha$ was obtained by comparing Bardon's thermal network to the one of his macroscopic thermal contact model (equations (1) and (2)), *figure 11(c)*. It gives:

$$\alpha = \frac{R_{sl2}}{R_{sl2} + R_{sl1}} \tag{19}$$

In our microscopic models, friction heat is generated in a volume defined the two heights $h_1$ and $h_2$. It has been verified that if $h_1$ and $h_2$ tend toward zero (i.e., the volumic heat generation tends to a surface heat generation), the numerical value of $\alpha$ obtained from the numerical methodology (Section 2.4.2) tends toward the value given by equation (19).

In this section, an analytical expression for $\alpha$ which includes the volumetric friction heat generation parameters is developed. The aim is to better understand the influence of each parameters and the physical significance of $\alpha$.

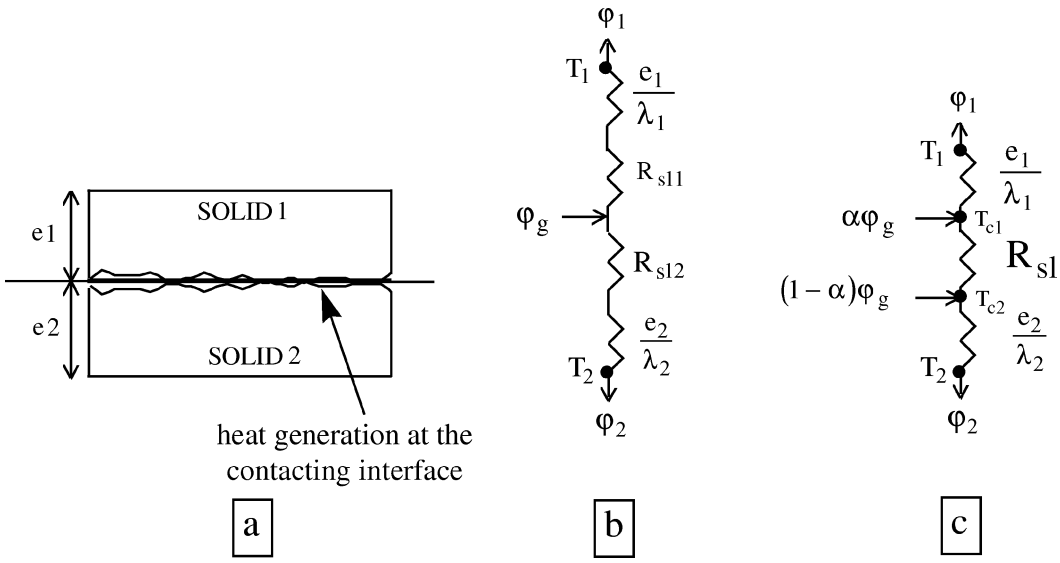


**Figure 11.** Equivalent thermal resistance network of two contacting solids for which friction heat is generated at the theoretical interface of contact. Application to the sliding contact thermal model proposed by Bardon [4].

### 4.1. General expression of $\alpha$

$\alpha$ depends on the same parameters than $R_{sl}$ (listed in the previous section), but it also depends on $w_i(h)$ and $g_i(h)$: the volume in which the friction heat is generated and the spatial variation of the friction heat, respectively.

It is demonstrated (see appendix) that if a friction heat, $d\varphi_{g2}(h)$, were only generated on a fictive interface, located in the solid 2 at a distance $h$ from the theoretical interface, then $\alpha$ noted to $\alpha_2(h)$ would be equal to:

$$\alpha_2(h) = \frac{R_{sl2}(1-\eta_2(h)) - h/\lambda_2}{R_{sl}} \qquad (20)$$

On the other hand, if a friction heat, $d\varphi_{g1}(h)$, were generated only on a fictive interface in the solid 1, then a similar procedure could be used to determine $\alpha$, noted $\alpha_1(h)$:

$$\alpha_1(h) = \frac{R_{sl2} + \eta_1(h)R_{sl1} + h/\lambda_1}{R_{sl}} \qquad (21)$$

As the thermal properties are not temperature dependent then the volumetric heat generation is the sum of these elementary heat generations distributed within the two solids. The value of $\alpha$ for the macroscopic sliding contact thermal model is such that:

$$\alpha\varphi_g = \int_0^{h_1} \alpha_1(h)\, d\varphi_{g1}(h) + \int_0^{h_2} \alpha_2(h)\, d\varphi_{g2}(h) \qquad (22)$$

The two functions $\eta_1(h)$ and $\eta_2(h)$ are dimensionless. They depend on the distance, $h$, between the theoretical and fictive interfaces. By definition $\eta_i(h)$ can vary between 0 and 1 but has no physical significance. Their value must be known to integrate equation (22). Recalling that the distance $h$ is the location of the fictive surface heat source, lets consider the two limiting cases:

– $\eta_i(h) = 0$ when $h = 0$, the friction heat is generated at the real contact interface only. Equation (20) or (21) can be directly used to determine $\alpha$ and it gives exactly the same expression than the one given by Bardon (equation (19)).

– $\eta_i(h) = 1$ when the fictive heat generation interface location is far from the real contact interface. Even if it is a theoretical configuration which might not occur in practical cases, it is still worth studying to point out that $\alpha$ is mathematically not bounded between 0 and 1.

As a matter of fact, if the friction heat were generated in solid 1 at a distance h far from the real contact interface and nowhere else, $\eta_1(h) = 1$ and equation (21) becomes:

$$\alpha_1(h) = 1 + \frac{h}{\lambda_1 R_{sl}} \qquad (23)$$

consequently, $\alpha_1(h)$, which in this case would be equal to $\alpha$, would be greater than 1.

Similarly, with $\eta_2(h) = 1$, equation (20) would lead to:

$$\alpha_2(h) = -\frac{h}{\lambda_2 R_{sl}} \qquad (24)$$

which indicates that if such a situation were to occur, $\alpha_2(h)$, which would be equal to $\alpha$, would be negative.

$\alpha$ is usually interpreted as the fraction of the friction heat generated at the surface of the solid 1 while the other part is generated at the surface of the solid 2 [8]. This interpretation naturally leads to the fact that $\alpha$ should be a real between 0 and 1. The two preceding cases will never happen because friction heat is always generated in a volume around the real contact interface in the two solids. They were only developed to explain (as shown further by the numerical example (Section 4.3)) that it is possible to have value of $\alpha$ outside the $[0, 1]$ interval. $\alpha$ is not a bounded real because it depends not only on the thermal contact resistance ($R_{sl1}$ and $R_{sl2}$, function of the defect's shape and solid thermal properties), but also, on the volumetric distribution of the friction heat described by $g_1$, $g_2$, $w_1$, $w_2$, $h_1$, $h_2$, $\eta_1$ and $\eta_2$.

## 4.2. Determination of the $\eta$ functions

The determination of $\eta_i(h)$ comes naturally from the numerical methodology presented in Section 2.4.2. To have numerical values of $\eta_i(h)$ it is necessary to consider a fictive interface in only one solid:

– If the fictive interface is within solid 2, then it is possible to calculate the thermal resistances ($R_{sl}$ and $R_{sl2}$) and $\alpha_2(h)$ with the numerical methodology and then use equation (20) to $\eta_2(h)$:

$$\eta_2(h) = 1 - \frac{R_{sl}\alpha_2(h)}{R_{sl2}} - \frac{h}{R_{sl2}\lambda_2} \qquad (25)$$

– If the fictive interface is within the solid 1, then it is possible to calculate the thermal resistances ($R_{sl1}$ and $R_{sl2}$) and $\alpha_1(h)$ with the numerical methodology and then use equation (21) to $\eta_1(h)$:

$$\eta_1(h) = -\frac{R_{sl2}}{R_{sl1}} + \frac{R_{sl}\alpha_1(h)}{R_{sl1}} - \frac{h}{R_{sl1}\lambda_1} \qquad (26)$$

## 4.3. Numerical examples

The aim of this section is to validate the analytical analysis which has lead to equation (22). To achieve this, the $\eta_i(h)$ are first determined (Section 4.2). Then, for a given volumetric friction heat generation, $\alpha$ is determined from integration of equation (22). This 'analytical' value is finally compared with the 'numerical' value obtained by the numerical solution of the microscopic models (Section 2.4.2). The R/R model is first considered and then the S/R model.

### 4.3.1. Results for the R/R model

A situation where solids 1 and 2 are identical is considered. The values of the geometrical and thermophysical parameters are:

$2B = 10$ µm; $\qquad 2b_1 = 2b_2 = 3$ µm;

$H_1 = H_2 = 4.2$ µm;

$\lambda_1 = \lambda_2 = 15\ \mathrm{W{\cdot}m^{-1}{\cdot}K^{-1}}$;

$\rho_1 = \rho_2 = 7700\ \mathrm{kg{\cdot}m^{-3}}$;

$cp_1 = cp_2 = 150\ \mathrm{J{\cdot}kg^{-1}{\cdot}K^{-1}}$; $\qquad V^* = 3.85$

As solids 1 and 2 are identical, the thermal resistances, $R_{sl1} = R_{sl2} = R_{sl}/2$ and $\eta_1(h) = \eta_2(h) = \eta(h)$. Use of numerical solution for the microscopic model and equations (15) and (9) gives:

$$R_{sl} = 2.52{\cdot}10^{-6}\ \mathrm{m^2{\cdot}K{\cdot}W^{-1}}$$

$\eta(h)$ is determined (Section 4.2. equations (25) and (26)) for $h$ varying between 0 and $2H$. Variations of $\eta(h)$ are presented as a function of the dimensionless height $h^* = h/2B$ on *figure 12*. As expected, $\eta(h)$ has an asymptotic value equal to 1.

To obtain an analytical expression of $\alpha$ equation (22) must be integrated. As explained in Section 1.3, $g_1(h)$ and $g_2(h)$ are supposed to be constant, i.e., it is supposed that heat is generated uniformly within each solid in a volume defined by $h_1$ and $h_2$. Then the calculation of the

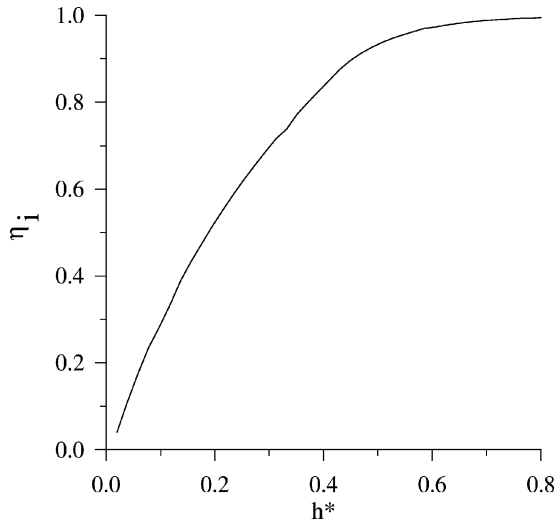


**Figure 12.** Variation of $h$ for the R/R model with the non-dimensional distance $h^*$ between the real contact interface and the fictive surface where the friction heat is generated.

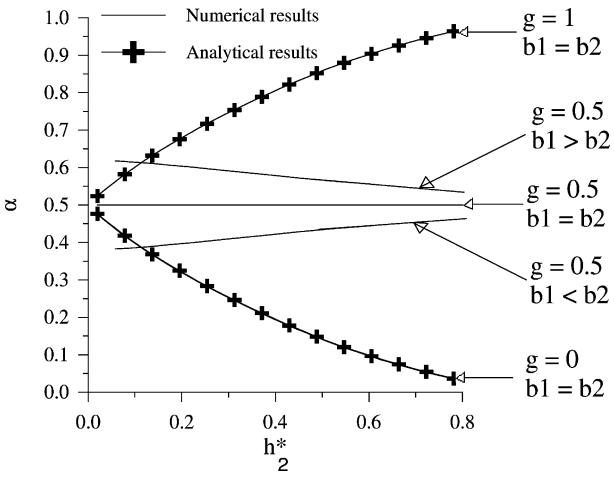


**Figure 13.** Analytical and numerical values of the friction heat generation factor a for the R/R microscopic model.

integrals of equation (22) is straightforward and $\alpha$ can be determined:

$$\alpha = \frac{1}{R_{sl}}\left[R_{sl2} - \bar{\eta}_2 R_{sl2} - \frac{h_2}{2\lambda_2} + g\left(R_{sl1}\bar{\eta}_1 + R_{sl2}\bar{\eta}_2 + \frac{1}{2}\left(\frac{h_1}{\lambda_1} + \frac{h_2}{\lambda_2}\right)\right)\right] \quad (27)$$

$$\text{with } \bar{\eta}_i = \frac{1}{h_i}\int_0^{h_i} \eta(h)\,\mathrm{d}h \quad (28)$$

This equation allows to calculate $\alpha$ for any values of $h_1$, $h_2$ and $g$ (fraction of the friction heat generated in the solid 1).

For example $\alpha$ is calculated for $g = 0$ (the friction heat is generated only in the solid 2) and $g = 1$ (the friction heat is generated only in the solid 1) for different values of $h_2^*$ and $h_1^*$, respectively. *Figure 13* compares these values with the ones determined from the numerical methodology (Section 2.4.2). There is no difference between the analytical and numerical results. The agreement between the two methods has been verified for other width, height, thermal properties and velocity, consequently only the analytical results are presented. These results really show that $\alpha$ depends on the location of the friction heat. Actually, values $g = 0$ and $g = 1$ may never occur since friction heat is usually generated in the two contacting solids. However it gives the interval of variation of $\alpha$ for this geometry ($b_2^* = b_1^*$).

Using equation (27), $\alpha$ is calculated for $g = 0.5$ (same friction heat generation in each solid), $h_2^* = h_1^*$ and three $(b_1^*, b_2^*)$ couples (*figure 13*):

– for $b_2^* = b_1^*$ the configuration is symmetrical for the two solids thus $\alpha = 0.5$.

– for $b_2^* > b_1^*$ the thermal resistance due to solid 2 is lower than the one due to solid 1 and, for this particular set of parameters, $\alpha$ is always lower than 0.5.

– the opposite is observed for $b_2^* > b_1^*$ since the thermal resistance due to solid 1 is lower than the one due to solid 2.

– the variations of $\alpha$ with $h^*$ are not very large since it is supposed that $h_2^* = h_1^*$ and $H_2^* = H_1^*$.

### 4.3.2. Results for the S/R model

The value of the geometrical and thermophysical parameters are:

$$2B = 10\ \mu\text{m}, \quad 2b_1 = 3\ \mu\text{m}, \quad H_1 = 8.4\ \mu\text{m},$$
$$\lambda_1 = \lambda_2 = 15\ \text{W·m}^{-1}\text{·K}^{-1}, \quad \rho_1 = \rho_2 = 7700\ \text{kg·m}^{-3},$$
$$cp_1 = cp_2 = 150\ \text{J·kg}^{-1}\text{·K}^{-1}$$

The dimensionless sliding velocity is equal to $V^* = 3.85$.

The thermal resistances, $R_{sl1}$ and $R_{sl2}$, due to solid 1 and 2 are not the same. The combination of equations (12), (13) and (9) leads to:

$$R_{sl} = 1.65{\cdot}10^{-6}\ \text{m}^2\text{·K·W}^{-1},$$
$$R_{sl1} = 1.50{\cdot}10^{-6}\ \text{m}^2\text{·K·W}^{-1},$$
$$R_{sl2} = 0.15{\cdot}10^{-6}\text{m}^2\text{·K·W}^{-1}$$

$\eta_1$ and $\eta_2$ differ and are determined for $h$ varying between 0 and $2H$. Variations of $\eta_i$ are shown as a function of the dimensionless height $h_i^* = h_i/2B$ on *figure 14*.

For the smooth solid, $\eta_2(h_2^*)$ seems to start from a value of 0.9 for $h_2^* = 0$. Due to numerical reason, $\eta_2(h_2^*)$ was not calculated for $h_2^* = 0$ but for a very small value of $h_2^*$. Moreover it has been shown in Section 4.1 that $\eta_2(h_i^*)$ must be equal to 0 for $h_2^* = 0$. This means that there is a tremendous increase of $\eta_2(h_2^*)$ for really small values of $h_2^*$ even if it is not represented on the graph.

The curve of $\eta_1(h_1^*)$ for the rough solid of the S/R is to be compared to the curve obtained for the R/R model (*figure 12*). The geometries considered for the two cases are the same. The two values of $\eta_1$ have an asymptotic value equal to 1 but for the S/R model $\eta_1$ soars for $h_1^* = H_1^*$ whereas $\eta_1$ increases gradually for the R/R model. This difference is due to the fact that for the R/R model the width of the volume in which the friction heat is generated is constant versus $h_1^*$ (*figure 5*), whereas for the S/R model, the width of the volume in which the

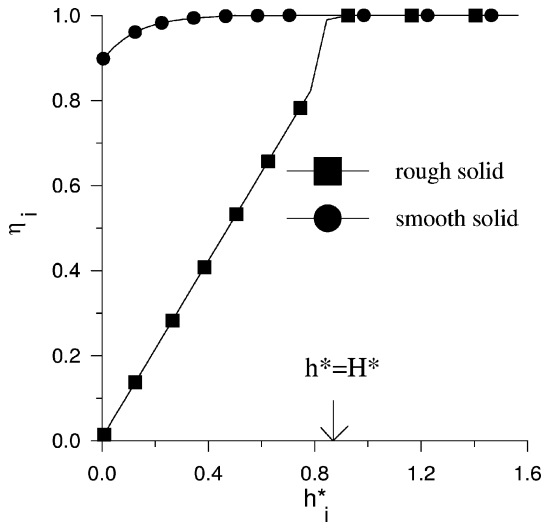


**Figure 14.** Value $h$ of the S/R model for the smooth and rough solids function of the non-dimensional distance $h^*$ between the real contact interface and the fictive surface where the friction heat is generated.

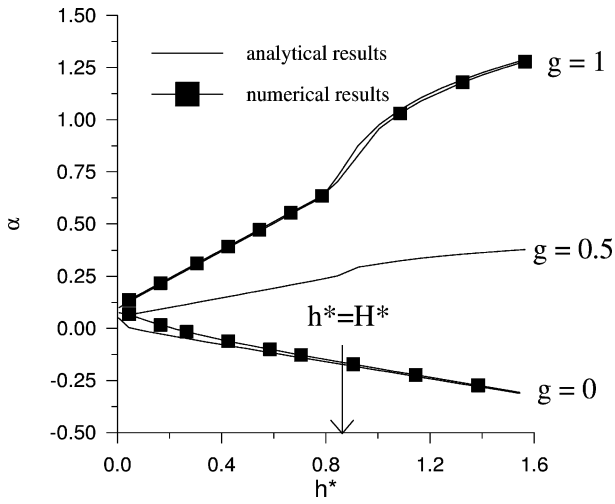


**Figure 15.** Analytical and numerical values of the friction heat generation factor a for the S/R microscopic model.

friction heat is generated is equal to $2b$ for $h_1^* < H_1^*$ and to $2B$ for $h_1^* > H_1^*$ (*figure 4*). It shows that the volume in which the friction heat is generated has an influence on $\eta_i$ and thus on the heat generation factor.

The two functions $g_1$ and $g_2$ which give the friction heat distribution in the two contacting solids are supposed to be constant. Then if $h_1 < H_1$ the integration of equation (22) gives the same results than for the R/R model and equation (27) is still usable. But if $h_1 > H_1$ the integration of equation (22) gives:

$$\alpha = \frac{1}{R_{sl}}\Bigg[R_{sl2} - \bar{\eta}_2 R_{sl2} - \frac{h_2}{2\lambda_2} + g^a\left(R_{sl1}\bar{\eta}_1^a + R_{sl2}\bar{\eta}_2 + \frac{1}{2}\left(\frac{H_1}{\lambda_1} + \frac{h_2}{\lambda_2}\right)\right) + g^b\left(R_{sl1}\bar{\eta}_1^b + R_{sl2}\bar{\eta}_2 + \frac{1}{2}\left(\frac{H_1 + h_1}{\lambda_1} + \frac{h_2}{\lambda_2}\right)\right)\Bigg] \tag{29}$$

where:

$$\bar{\eta}_2 = \frac{1}{h_2}\int_0^{h_2} \eta_2(h)\,\mathrm{d}h, \quad \bar{\eta}_1^a = \frac{1}{H_1}\int_0^{H_1} \eta_i(h)\,\mathrm{d}h \quad \text{and}$$

$$\bar{\eta}_1^b = \frac{1}{h_1 - H_1}\int_{H_1}^{h_1} \eta_i(h)\,\mathrm{d}h$$

$g^a$ is the fraction of the friction heat generated in solid 1 within the volume defined by $0 < h < H_1$,

$g^b$ is the fraction of the friction heat generated in solid 1 within the volume defined by $H_1 < h < h_1$.

Using equation (29), $\alpha$ is calculated for two particular cases:

– all the friction heat is generated in the solid 1 which means that $g = g^a + g^b = 1$.

– no friction heat is generated in the solid 1 which means that $g = 0$.

*Figure 15* allows to compare these values with the ones determined from the numerical methodology (Section 2.4.2). $\alpha$ is plotted versus the dimensionless height, $h^*$, i.e., the volume in which the friction heat is generated. *For* $g = 1$ the slight differences obtained for $h_1^* > H_1^*$ are due to the values of $\bar{\eta}_1^a$ and $\bar{\eta}_1^b$ which have been approximated to 0.5 and 1, respectively (*figure 14*). $\alpha$ increases with $h_1^*$ and becomes greater than 1. *For* $g = 0$, $\alpha$ is almost always negative. The differences between the numerical and analytical values are due to the lack of accuracy of $\eta_2$ for small value of $h_2^*$ (on *figure 14*), $\eta_2$ must be equal to 0 when $h_2^*$ is equal to 0) which leads to some errors when calculating $\bar{\eta}_2$. The difference vanishes when $h_2^*$ increases. These two curves give the range of variation of $\alpha$ for this particular geometry. One must keep in mind that they are not realistic since the friction heat is usually generated in the two solids. Thus the case $g = 0.5$ and $h_2^* = h_1^*$ is studied using equation (29) and the variations of $\alpha$ with $h^*$ is shown *figure 15*. It indicates that $\alpha$ is quite sensitive to $h^*$.

## 5. CONCLUSION

The total sliding contact resistance, and the friction heat generation factor (the two parameters of a macroscopic thermal contact model) were determined for two microcospic models. The geometry was chosen in order to implement simple numerical solutions to calculate thermal field in the sliding solids; they are not intended to accurately represent all real contacting surfaces, but they are used to point out the influence of the various parameters.

It was shown that the sliding resistances calculated from the two models can differ significantly, particularly when the ratio of the real to apparent contact area and the non dimensional velocity are small. Since the real contact area is usually much less than ten percent of the apparent contact area, the method that consists to transform a model with two rough surfaces into an equivalent model with a smooth and a rough surfaces [24, 31], must not be used for sliding contact.

It is the first time that the total sliding thermal contact resistance is determined numerically for two rough surfaces. For convenience, the correlation for $R_{\mathrm{sl}}$ has been developed.

The friction heat generation factor was also studied assuming that the friction heat is generated in a volume. Numerical values can be calculated using the numerical methodology. An analysis was conducted to built an analytical expression of the generation factor as a function of the microscopic parameters. It was shown that the generation factor depends not only on the conductive heat transfer in the solids in the vicinity of the interface, but also on the friction heat generation parameters (geometric parameters and heat flux distribution). The generation factor is mathematically not bounded and can be negative or greater than one. This study point out that it is important to understand better the mechanisms of friction heat generation since it influences $\alpha$, which in turn, influences the macroscopic surface temperatures of the rubbing bodies.

## APPENDIX: ANALYTICAL EXPRESSION OF $\alpha$ FOR FRICTION HEAT GENERATED ON A FICTIVE INTERFACE IN SOLID 2

Let consider on *figure 16(a)* the case of a local friction heat generation at a fictive interface in the solid 2 located at a distance $h$ from the real contact interface. This case is similar to one of *figure 11(a)*, thus the thermal resistance network shown *figure 16(b)* can be derived from *figure 11(b)*. The analogy with equation (19) allows to obtain a relation for $\alpha_2'(h)$:

$$\alpha_2'(h) = \frac{R_{\mathrm{sl2}}(h)}{R_{\mathrm{sl}}} = \frac{R_{\mathrm{sl2}}}{R_{\mathrm{sl}}}\big(1 - \eta_2(h)\big) \tag{30}$$

$\alpha_2'(h)$ is equal to the ratio of a thermal contact resistance between the fictive interface and the external surface of the solid 2, $R_{\mathrm{sl2}}(h)$, to the total sliding contact resistance $R_{\mathrm{sl}}$. In other words, $R_{\mathrm{sl2}}(h)$ is equal to $R_{\mathrm{sl2}}$ minus a fraction, $\eta_2(h)$, of $R_{\mathrm{sl2}}$, with $0 \leq \eta_2(h) \leq 1$.

This value of $\alpha_2'(h)$ allows to couple the two contacting solids at the *fictive interface* (*figure 16(c)*). The two coupling equations are obtained by analogy with equations (1) and (2):

$$\mathrm{d}\varphi_{\mathrm{g2}}(h) = \mathrm{d}\varphi_1 + \mathrm{d}\varphi_2, \tag{31}$$

$$\mathrm{d}\varphi_1 = \alpha_2'(h)\,\mathrm{d}\varphi_{\mathrm{g2}}(h) + \frac{T_{c2}' - T_{c1}'}{R_{\mathrm{sl}}} \tag{32}$$

where $\mathrm{d}\varphi_{\mathrm{g2}}(h)$ is the heat flux density generated at the fictive interface of thickness $\mathrm{d}h$:

$$\mathrm{d}\varphi_{\mathrm{g2}}(h) = \frac{1}{2B} g_2(h) w_2(h)\,\mathrm{d}h \tag{33}$$

and the two temperatures $T_{\mathrm{c1}}'$ and $T_{\mathrm{c2}}'$ are the extrapolated temperatures at the *fictive interface*:

$$T_{\mathrm{c2}}' = \mathrm{d}\varphi_2\left(\frac{e_2}{\lambda_2} - \frac{h}{\lambda_2}\right) + T_2, \tag{34}$$

$$T_{\mathrm{c1}}' = \mathrm{d}\varphi_1\left(\frac{e_1}{\lambda_1} + \frac{h}{\lambda_2}\right) + T_1 \tag{35}$$

Actually it is desired to couple the solids at the *real contact interface*, *figure 16(d)*, and the two coupling equations should be:

$$\mathrm{d}\varphi_{\mathrm{g2}}(h) = \mathrm{d}\varphi_1 + \mathrm{d}\varphi_2, \tag{36}$$

and:

$$\mathrm{d}\varphi_1 = \alpha_2(h)\,\mathrm{d}\varphi_{\mathrm{g2}}(h) + \frac{T_{\mathrm{c2}} - T_{\mathrm{c1}}}{R_{\mathrm{sl}}} \tag{37}$$

where the two temperatures $T_{\mathrm{c1}}$ and $T_{\mathrm{c2}}$ are the contact temperatures extrapolated at the *real contact interface*:

$$T_{\mathrm{c2}} = \mathrm{d}\varphi_2 \frac{e_2}{\lambda_2} + T_2, \tag{38}$$

$$T_{\mathrm{c1}} = \mathrm{d}\varphi_1 \frac{e_1}{\lambda_1} + T_1 \tag{39}$$

Using equations (32) and (37) it is possible to write:

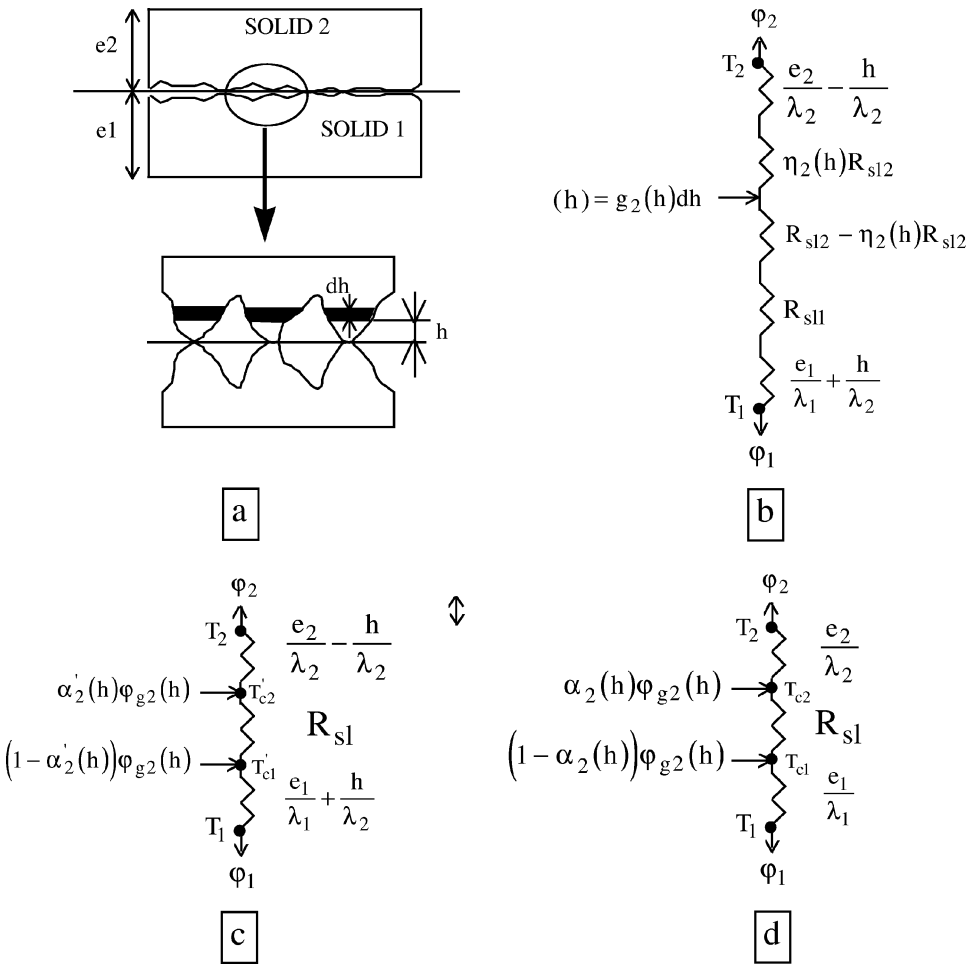


**Figure 16.** Equivalent thermal resistance network of two contacting solids for which friction heat is generated at a fictive interface of contact. Application to the determination of the friction heat generation factor using an analogy with the *figure 11*.

$$\alpha_2'(h)\,\mathrm{d}\varphi_{g2}(h) + \frac{T_{c2}' - T_{c1}'}{R_{sl}} = \alpha_2(h)\,\mathrm{d}\varphi_{g2}(h) + \frac{T_{c2} - T_{c1}}{R_{sl}} \qquad (40)$$

Where $T_{c1}'$, $T_{c2}'$, $\alpha_2'(h)T_{c1}$ and $T_{c2}$ are substituted by their expression given by equations (34), (35), (30), (38) and (39), respectively, which it leads to:

$$\alpha_2(h) = \frac{R_{sl2}(1-\eta_2(h)) - h/\lambda_2}{R_{sl}} \qquad (41)$$

## REFERENCES

[1] Block H., Theoretical study of temperature rise at surfaces of actual contact under oiliness lubricating conditions, in: Proceedings of the General Discussion on Lubrication and Lubricants, The Institute of Mechanical Engineers, London, England, Vol. 2, 1937, pp. 222–235.

[2] Kounas P.S., Dimarogonas A.D., The distribution of friction heat between a stationary pin and a rotating cylinder, Wear 19 (1972) 415–424.

[3] Berry F.R., Barber J.R., The division of frictional heat — a guide to the nature of sliding contact, J. Tribology 106 (1984) 405–415.

[4] Kennedy F.E., Ling F.F., A thermal, thermoelastic and wear simulation of a high energy sliding contact problem, J. Lubrication Technology (July 1974) 497–505.

[5] Kounas P.S., Dimarogonas A.D., The distribution of friction heat between a stationary pin and a rotating cylinder, Wear 19 (1972) 415–424.

[6] Malay K.K., Shyam Bahadur, Heat transfer analysis for a pin and disc sliding system, Wear 67 (1981) 71–84.

[7] Raynaud M., Bransier J., Estimation of friction heat partition at sliding contact using an inverse method, in:

Proceedings of the 9th Internat. Heat Transfer Conference, Vol. 3, Jerusalem, Israël, August 1990, pp. 151–156.

[8] Bardon J.P., Bases physiques des conditions de contact thermique imparfait entre milieux en glissement relatif, Rev. Générale de Thermique (1994) 85–92.

[9] Barber J.R., The conduction of heat from sliding solids, Internat. J. Heat Mass Transfer 13 (5) (1970) 857–871.

[10] Fletcher L.S., Recent developments in contact conductance heat transfer, J. Heat Transfer 110 (1988) 1059–1070.

[11] Lambert M.A., Fletcher L.S., Review of models for thermal contact conductance of metals, AIAA J. Thermophysics Heat Transfer 11 (2) (1997) 129–140.

[12] Beck J.V., Combined parameter and function estimation in heat transfer with application to contact conductance, ASME J. Heat Transfer 110 (1988) 1046–1058.

[13] Sadhal S.S., Unsteady heat flow between solids with partially contacting interface, ASME J. Heat Transfer 103 (1981) 32–35.

[14] Barber J.R., The effect of thermal distortion on constriction resistance, Internat. J. Heat Mass Transfer 14 (6) (1971) 751–766.

[15] Mazo L., Cassagne B., Badie Levet D., Bardon J.P., Etude des conditions de liaison thermiques dans le cas du frottement sec métal plastique, Rev. Générale de Thermique 204 (1978) 921–933.

[16] Li Y.H., Sellars C.M., Evaluation of interfacial heat transfer and its effects on hot forming process, Ironmaking and Steelmaking 23 (1996) 58–61.

[17] Malinowski Z., Lenard J.G., Davies M.E., A study of heat transfer coefficient as a function of temperature and pressure, J. Material Processing Technology 41 (1994) 125–142.

[18] Nshama W., Jeswiet J., Oosthuizen P.H., Evaluation of temperature and heat transfer conditions at the metal forming interface, J. Materials Procesing Technology 45 (1994) 637–642.

[19] Vinod K.J., Determination of heat transfer coefficient for forging applications, J. Material Shaping Technology 8 (1990) 193–202.

[20] Vullierme J.J., Lagarde J.J., Cordier H., Etude de la résistance de contact entre deux matériaux en frottement — influence de la vitesse de glissement, Internat. J. Heat Mass Transfer 22 (8) (1979) 1209–1219.

[21] Laraqi N., Influence de la vitesse de glissement sur la résistance thermique de constriction, Rev. Générale de Thermique 34 (408) (1995) 735–741.

[22] Laraqi N., Température de contact et coefficient de partage de flux généré par frottement sec entre deux solides. Approche nouvelle de la génération de flux, Internat. J. Heat Mass Transfer 35 (1992) 3131–3141.

[23] Greenwood J.A., Williamson J.B.P., Contact of nominally flat surfaces, Proc. Roy. Soc., Ser. A 295 (1440) (1966) 300–319.

[24] Salgon J.J., Robbe Valoire F., Blouet J., Bransier J., A mechanical and geometrical approach to thermal contact resistance, Internat. J. Heat Mass Transfer 40 (5) (1997) 1121–1130.

[25] Sridhar M.R., Yovanovich M.M., Review of elastic and plastic contact conductance models: comparison with experiments, J. Thermophysics Heat Transfer 8 (4) (1994) 633–640.

[26] Sadhal S.S., Unsteady heat flow between solids with partially contacting interface, Transactions of the ASME 13 (1981) 32–35.

[27] Kennedy F.E., Thermal and thermomechanichal effect in dry sliding, Wear 100 (1994) 453–476.

[28] Chantrenne P., Raynaud M., A microscopic thermal model for dry sliding contact, Internat. J. Heat Mass Transfer 40 (5) (1997) 1083–1094.

[29] Wanheim T., Petersen A.S., Theoretically determined model for friction in metal working processes, Wear 28 (1974) 251–258.

[30] Bardon J.P., Introduction à l'étude des résistances thermiques de contact, Rev. Générale de Thermique 125 (1972) 429–446.

[31] Johnson K.L., Contact Mechanics, Cambridge Univ. Press, Cambridge, 1985, p. 452.